


LETTER TO THE EDITOR

Open Access



DDX3X loss is an adverse prognostic marker in diffuse large B-cell lymphoma and is associated with chemoresistance in aggressive non-Hodgkin lymphoma subtypes

Atish Kizhakeyil^{1†}, Nurmahirah Binte Mohammed Zaini^{2†}, Zhi Sheng Poh^{1†}, Brandon Han Siang Wong¹, Xinpeng Loh³, Aik Seng Ng¹, Zun Siong Low¹, Praseetha Prasannan¹, Chun Gong⁴, Michelle Guet Khim Tan⁵, Chandramouli Nagarajan², Dachuan Huang⁶, Pang Wan Lu⁶, Jing Quan Lim⁶, Sharon Barrans⁷, Choon Kiat Ong^{6,8,9}, Soon Thye Lim^{10,11}, Wee Joo Chng^{12,13,14}, George Follows¹⁵, Daniel J. Hodson⁴, Ming Qing Du¹⁶, Yeow Tee Goh², Suat Hoon Tan¹⁷, Nicholas Francis Grigoropoulos^{2,8*†} and Navin Kumar Verma^{1,17*†} 

Keywords: DDX3X mutation, Hematolymphoid malignancy, Prognosis, Tumour metastasis, Drug resistance

Main text

Non-Hodgkin a diverse group of malignancies, encompassing the common diffuse large B-cell lymphoma (DLBCL) to the rarer T-cell lymphomas. Chemoresistance is a major barrier to treatment and the mechanisms through which it occurs are incompletely understood [1]. Although efforts are made to target frequently dysregulated pathways in NHL subtypes, these diseases still evolve into aggressive forms resistant even to newer therapies [2].

DEAD box helicase 3, X-linked (DDX3X) is an ATP-dependent RNA helicase and is involved in multiple

cancer-related cellular processes, including transcriptional regulation, cell adhesion, signal transduction and stemness [3]. It plays tumor suppressive or oncogenic roles depending on tumor type, and is implicated in various cancer types, including glioma, medulloblastoma, squamous cell carcinoma, hepatocellular carcinoma, lung and breast cancer [3]. A role for DDX3X in NHL subtypes remains unclear.

Here, we present our novel findings that *DDX3X* mutations are associated with poor prognosis in DLBCL. We demonstrate that mutation/loss of *DDX3X* in cell lines originated from DLBCL, cutaneous T-cell lymphoma (CTCL) and NK-cell/T-cell lymphoma (NKTCL) results in increased STAT3/p42/p44 phosphorylation and the development of chemoresistance. Intriguingly, *DDX3X* mutated/depleted B- and T-cell lineage NHL cell subtypes remain sensitive to pharmacological inhibitors of STAT3.

Recurrent *DDX3X* mutations in DLBCL are associated with worse clinical outcomes

Navigation through NHL patient samples in the cBioPortal [4] database revealed that *DDX3X* was mutated

*Correspondence: nicholas.francis.grigoropoulos@singhealth.com.sg; nkverma@ntu.edu.sg

[†]Atish Kizhakeyil, Nurmahirah Binte Mohammed Zaini and Zhi Sheng Poh contributed equally to this work.

[†]Nicholas Francis Grigoropoulos and Navin Kumar Verma are joint senior authors.

¹ Lee Kong Chian School of Medicine, Nanyang Technological University Singapore, 11 Mandalay Road, Clinical Sciences Building, Singapore 308232, Singapore

² Department of Haematology, Singapore General Hospital, The Academia, Level 3, 20 College Road, Singapore 169856, Singapore
Full list of author information is available at the end of the article



in 49 out of 1343 (3.6%) DLBCL cases. Moreover, available database in the ICGC [5] and the COSMIC [6] portals revealed mutations in *DDX3X* in 63 out of 1319 (4.7%) and 160 out of 5160 (3.1%) DLBCL cases, respectively. Besides DLBCL, *DDX3X* was also recurrently mutated in other NHL subtypes, including Burkitt lymphoma (BL) and NKTCL [7]. Altogether, we identified 165 missense, 81 truncating, and 3 in-frame indel mutational variants in the *DDX3X* in NHL subtypes (Fig. 1A). DLBCL patients with *DDX3X* mutations (14 cases out of 223 from 3 different cohorts) had significantly worse median overall survival (41.13 months) compared to cases with wild-type *DDX3X* (211.07 months) (Fig. 1B). The 5-year overall survival of DLBCL patients with *DDX3X* lesions was only 22% compared to 72% ($p=0.021$) for patients without *DDX3X* alterations (Fig. 1B). Data availability for other end-points, such as progression-free survival or event-free survival, was insufficient for a robust analysis. Notably, we found several other mutations that co-existed in *DDX3X* mutant DLBCL cases (Table S2).

We performed whole exome sequencing and detected *DDX3X* mutations in 4 out of 9 relapsed/refractory DLBCL patients treated with R-CHOP or similar regimens. Five damaging *DDX3X* mutations were identified (PolyPhen-2 score = 1, Table S1) in the catalytic domains - R296C and V375fs*8 in the “helicase ATP-binding” and R475C, R475H and R534H in the “helicase C-terminal” (Fig. 1C). Targeted sequencing of *DDX3X* on exons 8–15 in samples from 158 unselected DLBCL patients showed damaging *DDX3X* variants in 5 subjects (3, 95% confidence interval 1–7%) (Fig. 1C). All the identified

DDX3X mutations were confirmed somatic and occurred in residues that are highly conserved across various species. These data indicate that *DDX3X* mutations are important determinants of response to chemotherapy in DLBCL.

DDX3X mutation/loss in NHL cell subtypes increases resistance to antineoplastic drugs

To determine the functional role of *DDX3X* mutations in drug resistance, we stably expressed mutant *DDX3X*-R475C in U2392 cells using CRISPR knock-in technique [8] and knocked-down *DDX3X* in a panel of NHL cell lines [DLBCL (U2392, BJAB), BL (Raji), NKTCL (SNK1, SNK6, NKYS), and CTCL (HuT78, MJ, MyLa)] using *DDX3X*-targeted shRNA or siRNA (Fig. S1). Cells were treated with IC_{50} concentrations (of wild-type cells) of commonly used histone deacetylase (HDAC) inhibitors (vorinostat, panobinostat, trichostatin, romidepsin), STAT3 inhibitors (stattic, WP1066) or doxorubicin and cell viability was analyzed by MTS-based assay. We observed significant resistance to doxorubicin in *DDX3X*-mutant/depleted U2392 and BJAB cells and to HDAC inhibitors in HuT78 and SNK1 cells (Fig. 1D; Fig. S2). Importantly, *DDX3X*-mutant/depleted NHL cell subtypes remained sensitive to pharmacological STAT3 inhibition (Fig. 1D), although no synergism of drug action was identified in these cell-types as analyzed by determining “Combination Index” using checkerboard assay and the CompuSyn software (Fig. 1E). These results strongly support the clinical data suggesting that *DDX3X* mutations cause true chemoresistance and worse overall survival, rather than simply being surrogate markers in NHL subtypes, including DLBCL, NKTCL and CTCL.

(See figure on next page.)

Fig. 1 Mutational landscape of *DDX3X*, its clinical impact and the effect of *DDX3X* mutation/loss on proliferation, invasiveness and chemoresistance in NHL cell subtypes. **A** A lollipop plot showing mutations in the *DDX3X* gene in NHL that were identified using cancer-associated genomic databases from multiple repositories (cBioPortal, ICGC, COSMIC), published literature and OncoKB. **B** Kaplan-Meier survival analysis of DLBCL patients with or without mutations in the *DDX3X* gene showing overall survival. Available data in cBioPortal are from three different cohorts - the Diffuse Large B cell Lymphoma (DFCI, Nat Med 2018; $n=127$), Diffuse Large B-Cell Lymphoma (TCGA, PanCancer Atlas; $n=48$), and Lymphoid Neoplasm Diffuse Large B-cell Lymphoma (TCGA, Firehose Legacy; $n=48$); accessed on 14 September 2021. Patients under the the Diffuse Large B cell Lymphoma (DFCI, Nat Med 2018) cohort were treated with R-CHOP like chemotherapy, whereas treatment information for patients under the other two cohorts is not available. **C** A mutational lollipop plot depicting 6 different mutations identified in R/R-DLBCL patients ($n=9$) using whole exome sequencing and 4 different mutations identified in unselected DLBCL patients ($n=158$) using targeted sequencing of exons 8–15. **D** Point mutation in *DDX3X* (*DDX3X*-R475C) in U2392 cells was created using CRISPR knock-in technique and *DDX3X* was depleted in U2392, BJAB HuT78 and SNK1 cell lines by nucleofecting with specific shRNA or siRNA (WT, wild-type; CTL, control; Mock, non-specific siRNA). These cells were incubated with IC_{50} concentrations (of WT cells as indicated) of vorinostat, panobinostat, trichostatin, romidepsin, stattic, WP1066, or doxorubicin for 48 h. Cell viability was accessed by the MTS-based assay. **E** Cells, as described in “D”, were treated with a varying combinations of vorinostat and WP1066 and their effects on cell viability were determined and tabulated in terms of “Combination Index”. **F** The effect of *DDX3X* mutation/knockdown on cell proliferation rates in U2392, HuT78 and SNK1 cells were determined by measuring cell viability using MTS-based assay at multiple time-points up to 1 week. **G** Control or *DDX3X*-mutant/depleted U2392, HuT78 and SNK1 cells were serum starved and allowed to transmigrate through Matrigel towards 10% human serum-enriched medium in the trans-well plates for up to 4 h. Cell migration was automatically quantified using impedance-based measurements in real-time by xCELLigence Real Time Cell Analyzer. Data represent 3 independent experiments and values in graphs are mean \pm SEM. **, $p < 0.01$ *, $p < 0.05$; ns, non-significant

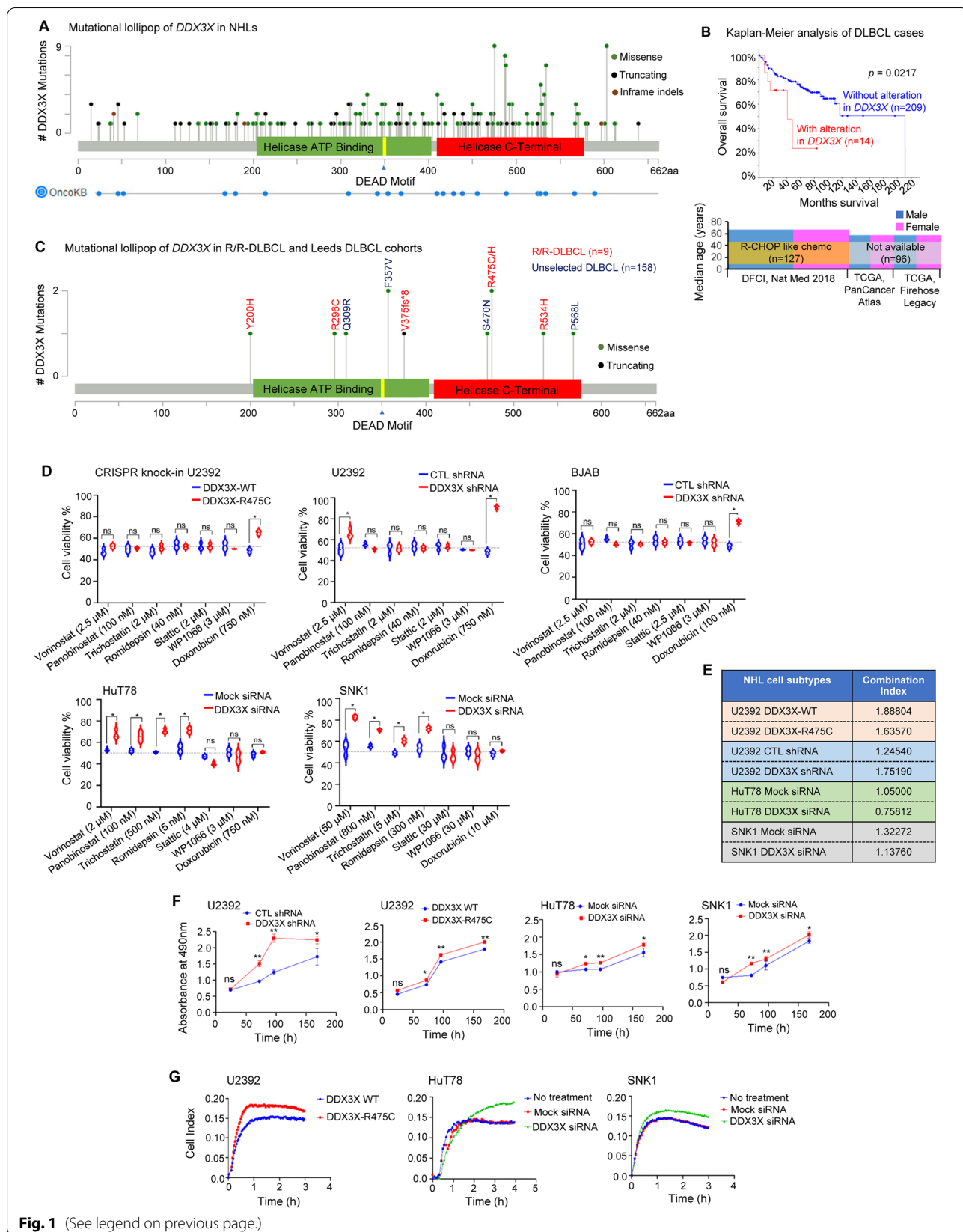


Fig. 1 (See legend on previous page.)

DDX3X mutation/loss enhances proliferation and migratory potential of NHL cell subtypes

DDX3X mutation/depletion in U2932, HuT78 and SNK1 cells significantly increased their proliferation rates in comparison to controls, as determined by MTS-based assay over 7 days (Fig. 1F). In contrast, forced overexpression of wild-type DDX3X in U2932 and HuT78 cells significantly decreased proliferation (Fig. S3). Real-time monitoring of cells transmigrating through Matrigel, using impedance-based measurements, showed significantly increased migratory/invasive potentials of DDX3X-mutant/depleted NHL cell subtypes (U2932, HuT78 and SNK1) (Fig. 1G). Western immunoblot analysis of DDX3X-mutant/depleted U2932 and HuT78 cells detected increased vimentin expression in these cell-types (Fig. S4). Overexpression of vimentin has been associated with aggressive transformation in lymphoma [9].

DDX3X mutation/loss in NHL subtype-derived cells increase cyclin-D1 expression

To further investigate the role of DDX3X in NHL subtypes, we carried out whole RNA-seq analysis of mutant DDX3X-R475C U2932, DDX3X-depleted HuT78 and DDX3X-depleted SNK1 cells in comparison to their wild-type and identified 451, 1682 and 441 differentially expressed genes (DEGs), respectively (Fig. 2A; Table S3-S5). We next performed gene network analysis using IPA® (a web-based application that enables analysis, integration, and interpretation of RNA-seq and other 'omics' datasets), DAVID (a biological module-centric algorithm that functionally analyzes large gene lists), and GSEA (an analytical method that determines whether an a priori defined gene sets shows significant differences between two biological states). This multimodal analysis of DEGs showed that DDX3X mutation/loss in NHL cells enriched cyclin-D1 and JAK-STAT3 pathways (Fig. 2B; Fig. S5; Table S6). Using RT-qPCR and

Western-immunoblot analysis, we verified that cyclin-D1 mRNA and protein levels were significantly elevated in DDX3X-mutant/depleted U2932 and Raji cells relative to control (Fig. 2C,D; Fig. S6). A subset of NHL patients, including 2.1% of DLBCL cases, has been found to overexpress cyclin-D1 [10] and the upregulation of cyclin-D1 has been associated with doxorubicin resistance in gastric cancer [11].

DDX3X mutation/loss in NHL cells enhances STAT3/MAPK activation

STAT3 and MAPK are well-studied oncogenes, known to inhibit apoptosis and decrease response to cytotoxic agents [12]. Western immunoblot analysis of DDX3X-mutated/depleted cell lines derived from DLBCL (U2932), NKTCL (SNK1, SNK2) and CTCL (HuT78, MJ, MyLa) showed significantly enhanced expression of phosphorylated STAT3 (Fig. 2E). Notably, NKYS cells express mutant STAT3 with high levels of baseline activity that did not increase further. STAT3 knockdown did not affect DDX3X expression levels nor did STAT3 directly interact with DDX3X (Fig. S7), suggesting that STAT3 hyperphosphorylation is a downstream effect of *DDX3X* lesions. Moreover, DDX3X mutation/depletion in NHL subtypes (DLBCL, NKTCL, CTCL) significantly increased the phosphorylation of p42/44 MAPK (Fig. 2E). STAT3/p42/p44 pathways are thus likely to be key mediators of the tumorigenic effects of *DDX3X* mutations in the NHL subtypes studies. Xenografted mutant DDX3X-R475C U2932 cells showed comparable sensitivity to the STAT3 inhibitor WP1066 in vivo in comparison to wild-type U2932 cells into the NOD.Cg-Prkdc^{scid}Il2rg^{tm1Wjll} mice (Fig. 2F).

Conclusions

Despite being uncommon, the biological effects *DDX3X* mutations/loss in DLBCL and other NHL subtypes (NKTCL, CTCL), suggest a worse overall survival.

(See figure on next page.)

Fig. 2 RNA-seq and protein network analysis of DDX3X mutant/depleted NHL cell subtypes and the molecular effect of DDX3X mutation/loss on DLBCL, NKTCL and CTCL cell lines. **A** Volcano plots showing DEGs in DDX3X-R475C mutant U2932, and DDX3X-depleted HuT78 and SNK1 cells (false discovery rate < 0.05 and $p < 0.05$) as analysed by RNA-seq ($n = 3$ each). Gene Ontology functional mapping of DEGs are shown in the corresponding insets. **B** Molecular interaction networks of DEGs that were identified by RNA-seq analysis of the above DDX3X-mutant/depleted cell lines, as predicted by the IPA®. Symbols representing protein types and their predicted relationships are provided in the legends. Solid and dashed lines represent direct and indirect interactions, respectively. **C** The mRNA levels of cyclin-D1 (*CCND1*) in U2932 cells expressing mutant DDX3X-R475C (left panel) or transfected with DDX3X shRNA (right panel) were quantified by RT-qPCR (WT, wild-type; CTL, control). **D** Cyclin-D1 expression levels in U2932 cells expressing mutant DDX3X-R475C (left panel) or transfected with DDX3X shRNA (right panel) were quantified by Western immunoblotting. Relative densitometry graphs quantifying cyclin-D1 expression are presented. **E** Control or DDX3X-mutant/depleted cell lines of DLBCL (U2932), NKTCL (SNK1, SNK6, NKYS) and CTCL (HuT78, MJ, MyLa) were analysed by Western immunoblotting to determine phosphorylation levels of STAT3 and p42/44. Relative densitometry graphs quantifying the expression levels of indicated proteins are presented. **F** U2932 cells with wild-type DDX3X or CRISPR knock-in mutant DDX3X-R475C were subcutaneously injected into NOD.Cg-Prkdc^{scid}Il2rg^{tm1Wjll} mice. Cells were left to grow for 3 weeks to develop into tumors. Xenografted mice were then injected (intra-tumoral) with vehicle or WP1066 (40 mg/kg) every 3 days for up to Day-58. Tumor volume (mm²) on each mice was recorded twice/week by caliper measurements and calculated by the modified ellipsoidal formula. $n = 5$ under each group. Data represent at least three experiments and values in graphs are mean \pm SEM. ***, $p < 0.001$; **, $p < 0.01$; *, $p < 0.05$; ns, non-significant

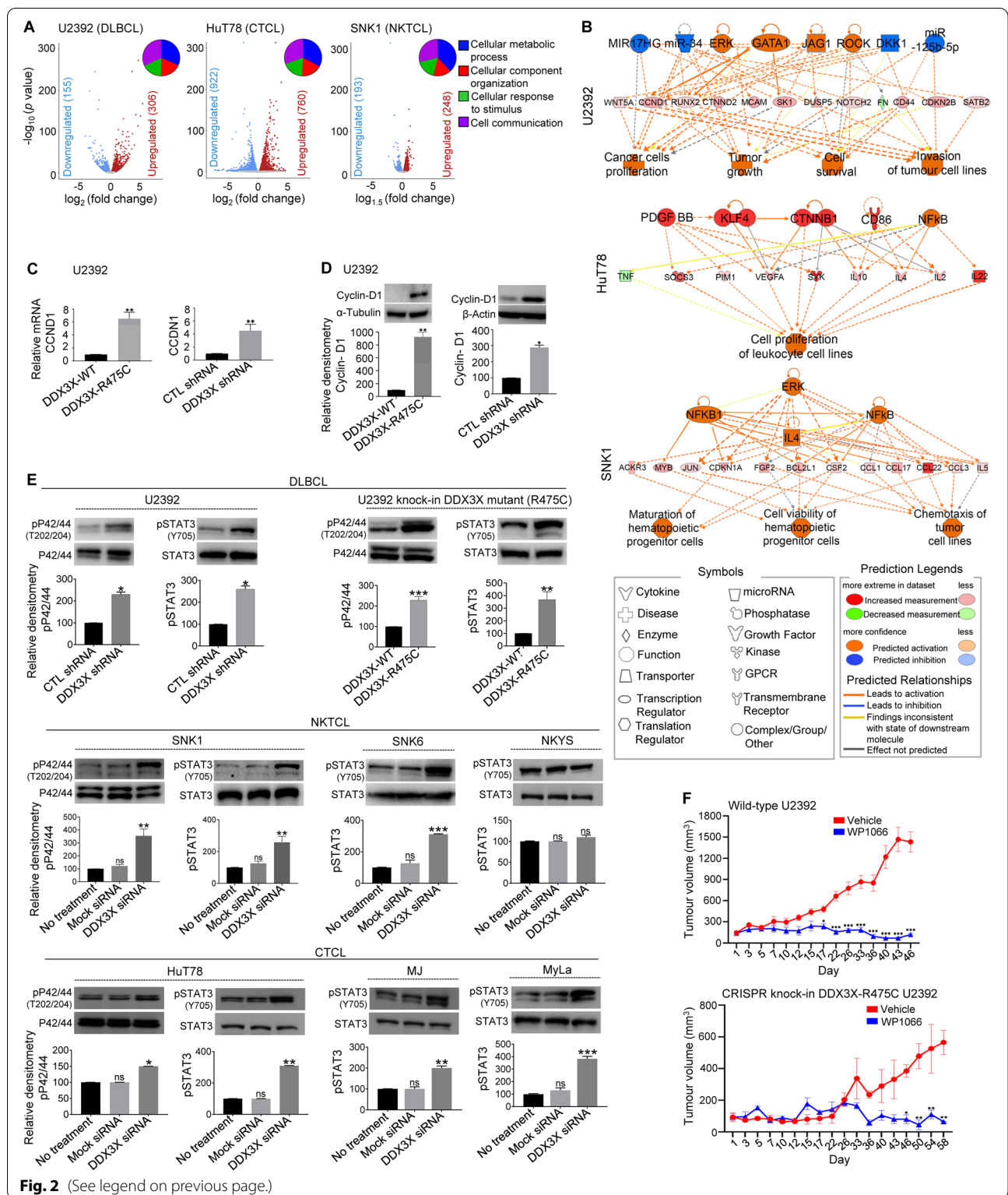


Fig. 2 (See legend on previous page.)

Given the high incidence of DLBCL [13, 14], the absolute number of patients with mutated *DDX3X* is likely to be substantial. Our results also suggest that STAT3

inhibition may be a rational choice for chemoresistant NHL (DLBCL, NKTCL, CTCL) patients with mutated *DDX3X*. The STAT3 inhibitor AZD9150 is currently in

phase 1b clinical trial in a subset of patients with heavily pre-treated lymphoma [15]. Further studies are needed to improve our understanding of the consequences of *DDX3X* mutation/loss, which would help improve risk stratification of aggressive NHL subtypes and identify new therapeutic options for patients with poor prognosis.

Abbreviations

BL: Burkitt lymphoma; CTCL: Cutaneous T-cell lymphoma; DDX3X: DEAD box helicase 3, X-linked; DLBCL: Diffuse large B-cell lymphoma; HDAC: Histone deacetylase; NHL: Non-Hodgkin lymphoma; NKTL: Natural Killer/T-cell lymphoma.

Supplementary Information

The online version contains supplementary material available at <https://doi.org/10.1186/s12943-021-01437-0>.

Additional file 1: Supplementary Fig. 1. RNAi-mediated depletion of *DDX3X* in selected NHL cell lines. The above indicated NHL cell lines and primary T-cells were nucleofected with *DDX3X* siRNA or Mock siRNA (control) and incubated for 72 h. Few cell lines were stably transfected with *DDX3X* shRNA or control (*CTL*) shRNA (as indicated) and were induced to knockdown *DDX3X*. In addition, U2392 cells were induced to express mutant *DDX3X*-R475C using CRISPR knock-in technique. **(A)** Cellular lysates from control and *DDX3X*-depleted/mutant cells were Western immunoblotted for quantifying *DDX3X* protein expression. Blots were re-probed for GAPDH or β -actin as loading control. **(B)** Relative levels of *DDX3X* mRNA were evaluated using quantitative reverse transcription PCR (RT-qPCR). Values in the RT-qPCR bar graphs are mean \pm SEM. Results represent at least 3 independent experiments. **, $p < 0.01$. **Supplementary Fig. 2.** Consequence of *DDX3X* loss on refractoriness of HuT78 cells towards the effect of vorinostat. HuT78 cells were nucleofected with *DDX3X* siRNA or Mock siRNA (control) and after 48 h, cells were incubated with vorinostat (IC_{50}). Cells were analyzed using MTS assay for cell viability **(A)** and Annexin-V/PI staining with subsequent flow-cytometry for apoptosis **(B)**. Cell lysates were collected and Western immunoblotted for determining the expression levels of *DDX3X*, cleaved PARP, and cleaved caspase 3 **(C)**. Blots were re-probed with anti-GAPDH to confirm equal loading. Values are mean \pm SEM and results represent at least 3 independent experiments. **, $p < 0.01$; ***, $p < 0.001$; ****, $p < 0.0001$.

Supplementary Fig. 3. Effect of *DDX3X* overexpression on the rate of proliferation of CTCL and DLBCL cells. HuT78 and U2392 cells were nucleofected with plasmid containing wild-type *DDX3X* (*DDX3X OE*) or vector alone. The overexpression of *DDX3X* in HuT78 **(A)** and U2392 **(B)** cells was confirmed by Western immunoblotting. Relative densitometry graphs of *DDX3X* in both cell types are shown. **(C)** The rate of HuT78 cell proliferation was determined by MTS-based assay, performed in triplicates at 48 h and 96 h. **(D)** The viability of U2392 cells was determined by MTS-based assay, performed in triplicates at 48 h. Values are mean \pm SEM and results represent at least 3 independent experiments. *, $p < 0.05$; **, $p < 0.01$.

Supplementary Fig. 4. Effect of the modulation of *DDX3X* expression on the expression levels of vimentin in CTCL and DLBCL cells. **(A)** HuT78 cells were nucleofected with *DDX3X* siRNA or Mock siRNA (control) and then lysed after 72 h. **(B)** *DDX3X* wild-type (*WT*, control) and CRISPR knock-in mutant *DDX3X*-R475C U2392 cells were lysed. **(C)** U2392 cells transfected with control (*CTL*) or *DDX3X* shRNA were lysed. **(D)** HuT78 cells were nucleofected with plasmid containing wild-type *DDX3X* (*DDX3X OE*) or vector alone and then lysed after 72 h. **(E)** U2392 cells were nucleofected with plasmid containing *DDX3X OE* or vector alone and then lysed after 48 h. All the cellular lysates (as indicated in the figure panels) were Western immunoblotted for quantifying the expression levels of vimentin. Blots were re-probed for GAPDH as loading control. Data represent at least 3 independent experiments. Values are mean \pm SEM; **, $p < 0.01$; *, $p < 0.05$. **Supplementary Fig. 5.** Gene-set enrichment analysis (GSEA) of *DDX3X*-mutant/depleted DLBCL, CTCL and NKTL cells. Genomic data

from *DDX3X*-R475C mutant U2392 **(A)**, *DDX3X*-depleted HuT78 **(B)**, and *DDX3X*-depleted SNK1 **(C)** cells were analyzed by GSEA. Hallmark gene sets (H) and oncogenic signature (C6) gene sets were collected from the Molecular Signatures Database (MSigDB) to produce the enrichment plots. p -values were calculated by 1000-gene-set two-sided permutation tests. **Supplementary Fig. 6.** Upregulation of cyclin-D1 in BL cells upon *DDX3X* depletion. Control and *DDX3X*-depleted Raji cells (using *shRNA#1* or *shRNA#2*) were lysed, and cellular lysates were analyzed for the expression levels of *DDX3X* and cyclin-D1 by Western immunoblotting. Blots were re-probed with anti- β -actin to confirm equal loading. Data represent at least 3 independent experiments. Values in the relative densitometry graphs are mean \pm SEM; *, $p < 0.05$. **Supplementary Fig. 7.** Effect of *DDX3X* loss on STAT3 regulation in CTCL cells. **(A)** HuT78 cells were treated with *DDX3X* siRNA and STAT3 GapmeR. Cellular lysates were collected and Western immunoblotted to determine the expression levels pSTAT3(Y705), STAT3, *DDX3X*, and GAPDH (loading control). Relative densitometry graph of immunoblots is presented. *, $p < 0.01$. **(B)** Cell lysates of HuT78 cells were immuno-precipitated (*IP*) using anti-*DDX3X* antibody or IgG control. Subsequently the immuno-precipitates were resolved on SDS-PAGE and subjected to immunoblotting with anti-STAT3 and anti-*DDX3X* antibodies. Data represent at least 3 independent experiments.

Additional file 2: Supplementary Table 1. Details of somatic mutations identified in 9/167 patients with DBCL.

Additional file 3: Supplementary Table 2. A list of mutated genes that co-existed in DLBCL patients with *DDX3X* mutations. **Supplementary Table 3.** A list of DEGs in *DDX3X*-R475C mutant vs wild-type U2392 cells. **Supplementary Table 4.** A list of DEGs in *DDX3X*-depleted vs control HuT78 cells. **Supplementary Table 5.** A list of DEGs in *DDX3X*-depleted vs control SNK1 cells. **Supplementary Table 6.** Top 10 biological pathways based on DAVID and IPA.

Acknowledgements

Authors acknowledge Dr. George Vassiliou and Dr. Niccolo Bolli, Wellcome Sanger Institute, Wellcome Genome Campus, Hinxton, UK for assistance with WES. We thank Professor Andrew Jack, HMDS, Leeds Cancer Centre for providing DNA samples from DLBCL cases.

Authors' contributions

The study was conceptualized by N.K.V. and N.F.G. with input from W.J.C., S.T.L., and C.K.O. Experiments were performed by A.K., N.B.M.Z., Z.S.P., B.H.S.W., X.L., A.S.N., P.P., P.W.L., J.Q.L., D.H., and S.B. under the supervision of N.K.V., S.H.T. and N.F.G. Bioinformatical analysis was performed by A.K., Z.S.P., and Z.S.L. Patient tumor samples and reagents were supplied by N.F.G., D.J.H., S.B. and C.G. Results were analysed and interpreted by N.K.V., N.F.G., M.Q.D., Y.T.G., M.G.K.T., C.N., G.F. and S.H.T. Figures were prepared by A.K. and Z.S.P. The manuscript was written by A.K., N.K.V. and N.F.G. All authors read and agreed to the final version of the manuscript.

Funding

This research was supported, in part, by Start-Up Grant to NKV provided by Lee Kong Chian School of Medicine, Nanyang Technological University Singapore (L0412290), the Singapore Ministry of Education (MOE) under its MOE Academic Research Fund (AcRF) Tier 2 Grant (MOE2017-T2-2-004), and the National Research Foundation Singapore under its Open Fund Large Collaborative Grant (OFLCG18May-0028) and administered by the Singapore Ministry of Health's National Medical Research Council (NMRC). N.F.G. acknowledges funding support from the Singapore Ministry of Health's National Medical Research Council under its NMRC of Singapore Transition Award (NMRC/TA/0051/2016), Kay Kendall Leukaemia Fund Junior Clinical Research Training Fellowship (KKL649) and the Addenbrooke's Charitable Trust Research Training Fellowship. D.H. was supported by the Medical Research Council (MR/M008584/1) and Blood Cancer UK and receives core funding from Wellcome (203151/Z/16/Z) and MRC to the Wellcome-MRC Cambridge Stem Cell Institute and from the CRUK Cambridge Centre (A25117). A.K. and Z.S.P. were provided with PhD fellowship by Lee Kong Chian School of Medicine, Nanyang Technological University Singapore. B.H.S.W. was provided with PhD fellowship by HealthTech NTU, Nanyang Technological University Singapore.

Availability of data and materials

RNA-seq data is publically available from the NCBI with GEO Accession #GSE163817. Other datasets are provided in the additional files.

Declarations**Ethics approval and consent to participate**

The study with patient tumor samples was approved by the ethics review board of Cambridge University Hospitals NHS Foundation Trust (05/Q1604/10) and conducted in accordance with the Declaration of Helsinki. Experiments utilizing primary lymphocytes were approved by the Nanyang Technological University Singapore Institutional Review Board (IRB-2018-05-034 and IRB-2014-09-007) and the SingHealth Central Institutional Review Board (201506–0069). Animal experiments were approved by the SingHealth Institutional Animal Care and Use Committee (IACUC No: 2016/SHS/1231).

Consent for publication

All authors give consent for the publication of manuscript in *Molecular Cancer*.

Competing interests

The authors declare that they have no competing interests.

Author details

¹Lee Kong Chian School of Medicine, Nanyang Technological University Singapore, 11 Mandalay Road, Clinical Sciences Building, Singapore 308232, Singapore. ²Department of Haematology, Singapore General Hospital, The Academia, Level 3, 20 College Road, Singapore 169856, Singapore. ³School of Biological Sciences, Nanyang Technological University Singapore, 60 Nanyang Dr, Singapore 637551, Singapore. ⁴Wellcome MRC Cambridge Stem Cell Institute, Cambridge, UK. ⁵Clinical Translational Sciences, Singapore General Hospital, The Academia Level 9, 20 College Road, Singapore 169856, Singapore. ⁶Lymphoma Genomic Translational Research Laboratory, Division of Cellular and Molecular Research, National Cancer Centre Singapore, 11 Hospital Drive, Singapore 169610, Singapore. ⁷Haematological Malignancy Diagnostic Service (HMDS), St. James's Institute of Oncology, Leeds, UK. ⁸Cancer and Stem Cell Biology, Duke-NUS Medical School, 8 College Road, Singapore 169857, Singapore. ⁹Genome Institute of Singapore, 60 Biopolis Street Genome, Singapore 138672, Singapore. ¹⁰Director's office, National Cancer Centre Singapore, 11 Hospital Drive, Singapore 169610, Singapore. ¹¹Office of Education, Duke-NUS Medical School, 8 College Road, Singapore 169857, Singapore. ¹²National University Cancer Institute, Singapore, Singapore. ¹³Cancer Science Institute of Singapore, National University of Singapore, Singapore, Singapore. ¹⁴NUS Center for Cancer Research (N2CR) and Dept of Medicine, Yong Loo Lin School of Medicine, National University of Singapore, Singapore, Singapore. ¹⁵Addenbrooke's Hospital NHS Foundation Trust, Cambridge, UK. ¹⁶Department of Pathology, University of Cambridge, Cambridge, UK. ¹⁷National Skin Centre Singapore, 1 Mandalay Road, Singapore 308205, Singapore.

Received: 27 July 2021 Accepted: 24 September 2021

Published online: 16 October 2021

References

- Coiffier B, Sarkozy C. Diffuse large B-cell lymphoma: R-CHOP failure-what to do? *Hematol Am Soc Hematol Educ Program*. 2016;2016:366378.
- Bakhshi TJ, Georgel PT. Genetic and epigenetic determinants of diffuse large B-cell lymphoma. *Blood Cancer J*. 2020;10:123.
- Mo J, Liang H, Su C, Li P, Chen J, Zhang B. DDX3X: structure, physiologic functions and cancer. *Mol Cancer*. 2021;20:38.
- Gao J, Aksoy BA, Dogrusoz U, Dresdner G, Gross B, Sumer SO, et al. Integrative analysis of complex cancer genomics and clinical profiles using the cBioPortal. *Sci Signal*. 2013;6:269.
- International Cancer Genome Consortium, Hudson TJ, Anderson W, Artez A, Barker AD, Bell C, et al. International network of cancer genome projects. *Nature*. 2010;464:993–8.
- Tate JG, Bamford S, Jubb HC, Sondka Z, Beare DM, Bindal N, et al. COSMIC: the catalogue of somatic mutations in cancer. *Nucleic Acids Res*. 2019;47:D941–7.
- Jiang L, Gu ZH, Yan ZX, Zhao X, Xie YY, Zhang ZG, et al. Exome sequencing identifies somatic mutations of DDX3X in natural killer/T-cell lymphoma. *Nat Genet*. 2015;47:1061.
- Gong C, Krupka JA, Gao J, Grigoropoulos NF, Giotopoulos G, Asby R, et al. Sequential inverse dysregulation of the RNA helicases DDX3X and DDX3Y facilitates MYC-driven lymphomagenesis. *Mol Cell*. 2021;81:4059–75. <https://doi.org/10.1016/j.molcel.2021.07.041>.
- Madsen C, Lauridsen KL, Plesner TL, Monrad I, Honoré B, Hamilton-Dutoit S, et al. High intratumoral expression of vimentin predicts histological transformation in patients with follicular lymphoma. *Blood Cancer J*. 2019;9:35.
- Ok CY, Xu-Monette ZY, Tzankov A, O'Malley DP, Montes-Moreno S, Visco C, et al. Prevalence and clinical implications of cyclin D1 expression in diffuse large B-cell lymphoma (DLBCL) treated with immunochemotherapy: a report from the international DLBCL rituximab-CHOP consortium program. *Cancer*. 2014;120:1818–29.
- Ji ZP, Qiang L, Zhang JL. Transcription activated p73-modulated cyclin D1 expression leads to doxorubicin resistance in gastric cancer. *Exp Ther Med*. 2018;15:1831–8.
- Liang F, Ren C, Wang J, Wang S, Yang L, Han X, et al. The crosstalk between STAT3 and p53/RAS signaling controls cancer cell metastasis and cisplatin resistance via the slug/MAPK/PI3K/AKT-mediated regulation of EMT and autophagy. *Oncogenesis*. 2019;8:59.
- Siegel RL, Miller KD, Jemal A. Cancer statistics, 2020. *CA Cancer J Clin*. 2020;70:7–30.
- Zelenetz AD, Gordon LI, Abramson JS, Advani RH, Bartlett NL, Caimi PF, et al. NCCN guidelines insights: B-cell lymphomas, version 3.2019. *J Natl Compr Cancer Netw*. 2019;17:650–61.
- Reilly MJ, McCoon P, Cook C, Lyne P, Kurzrock R, Kim Y, et al. STAT3 antisense oligonucleotide AZD9150 in a subset of patients with heavily pretreated lymphoma: results of a phase 1b trial. *J Immunother Cancer*. 2018;6:119.

Publisher's Note

Springer Nature remains neutral with regard to jurisdictional claims in published maps and institutional affiliations.

Ready to submit your research? Choose BMC and benefit from:

- fast, convenient online submission
- thorough peer review by experienced researchers in your field
- rapid publication on acceptance
- support for research data, including large and complex data types
- gold Open Access which fosters wider collaboration and increased citations
- maximum visibility for your research: over 100M website views per year

At BMC, research is always in progress.

Learn more biomedcentral.com/submissions

